Acta Crystallographica Section D
Biological Crystallography
ISSN 0907-4449

Metal-substituted derivatives of the rubredoxin from *Clostridium pasteurianum*

Megan Maher,[a]* Maddalena Cross,[b]‡ Matthew C. J. Wilce,[a]§ J. Mitchell Guss[a] and Anthony G. Wedd[b]

[a]School of Molecular and Microbial Biosciences, University of Sydney, New South Wales 2006, Australia, and [b]School of Chemistry, University of Melbourne, Parkville, Victoria 3010, Australia

‡ Current address: Department of Medicine, University of Melbourne, Royal Melbourne Hospital, Parkville, Victoria 3010, Australia.
§ Current address: Crystallography Centre, School of Biomedical and Chemical Sciences and School of Medicine and Dentistry, University of Western Australia, Crawley, Western Australia 6009, Australia.

Correspondence e-mail: m.maher@mmb.usyd.edu.au

Received 10 October 2003
Accepted 4 December 2003

PDB References: Ga^{III}Rd, 1r0f, r1r0fsf; Hg^{II}Rd, 1r0g, r1r0gsf; Co^{II}Rd, 1r0h, r1r0hsf; Cd^{II}Rd, 1r0i, r1r0isf; Ni^{II}Rd, 1r0j, r1r0jsf.

Five different metal-substituted forms of *Clostridium pasteurianum* rubredoxin have been prepared and crystallized. The single Fe atom present in the Fe(S-Cys)$_4$ site of the native form of the protein was exchanged in turn for Co, Ni, Ga, Cd and Hg. All five forms of rubredoxin crystallized in space group *R*3 and were isomorphous with the native protein. The Co-, Ni- and Ga-substituted proteins exhibited metal sites with geometries similar to that of the Fe form (effective D_{2d} local symmetry), as did the Cd and Hg proteins, but with a significant expansion of the metal–sulfur bond lengths. A knowledge of these structures contributes to a molecular understanding of the function of this simple iron–sulfur electron-transport protein.

1. Introduction

Rubredoxins (Rd) contain a single Fe(S-Cys)$_4$ site and are the simplest of iron–sulfur electron-transfer proteins. The Rd from *Clostridium pasteurianum* (Rd*Cp*) was the first to be isolated and characterized (Lovenberg & Sobel, 1965). While it has been assumed that Rds function in electron transfer, their specific roles have been identified in only a few systems. Rd is a cofactor of a terminal oxidase in the sulfate-reducing eubacterium *Desulfovibrio gigas* (Gomes *et al.*, 1997) and is involved in hydrogen oxidation in the nitrogen fixer *Azotobacter vinelandii* (Chen & Mortenson, 1992). In the aerobic bacterium *Acinetobacter calcoaceticus*, Rd is a cofactor in alkane degradation (Geissdorfer *et al.*, 1995). Significantly, Rd has recently been implicated in oxygen detoxification in anaerobic and microaerophilic microorganisms. The superoxide reductase from *Pyrococcus furiosus* is proposed to catalyze reduction (rather than dismutation) of superoxide to hydrogen peroxide, utilizing electrons from NADPH by way of NADPH:rubredoxin oxidoreductase and Rd (Jenney *et al.*, 1999).

The structure and properties of Rd*Cp* have been studied extensively, as its relative simplicity allows a quantitative approach to an understanding of its structure and function.

(i) It was one of the first proteins whose structure was determined and refined by X-ray diffraction (PDB code 5rxn; 1.2 Å resolution; Herriott *et al.*, 1970; Watenpaugh *et al.*, 1972, 1979). The resolution has been improved to 1.1 Å (PDB code 1iro; Dauter *et al.*, 1996), emphasizing the pseudo-twofold symmetry at the active site (effective D_{2d} local symmetry; Fig. 1).

(ii) This relative simplicity has allowed detailed study of the molecular factors that determine the potential of the Fe^{III}/Fe^{II} couple (Xiao & Wedd, 2001). The primary and secondary coordination spheres have been altered systematically by metal substitution and site-directed mutagenesis (Meyer *et al.*,

1995; Xiao *et al.*, 1998, 2000; Eidsness *et al.*, 1999; Maher *et al.*, 1999; Lin *et al.*, 2003). Most recently, we have reported Rd*Cp* mutants incorporating an exchangeable coordination position that allows construction of $Fe_2^{III}S_2$ and $(S\text{-}Cys)_3Fe^{III}OH$ centres (Cross *et al.*, 2002).

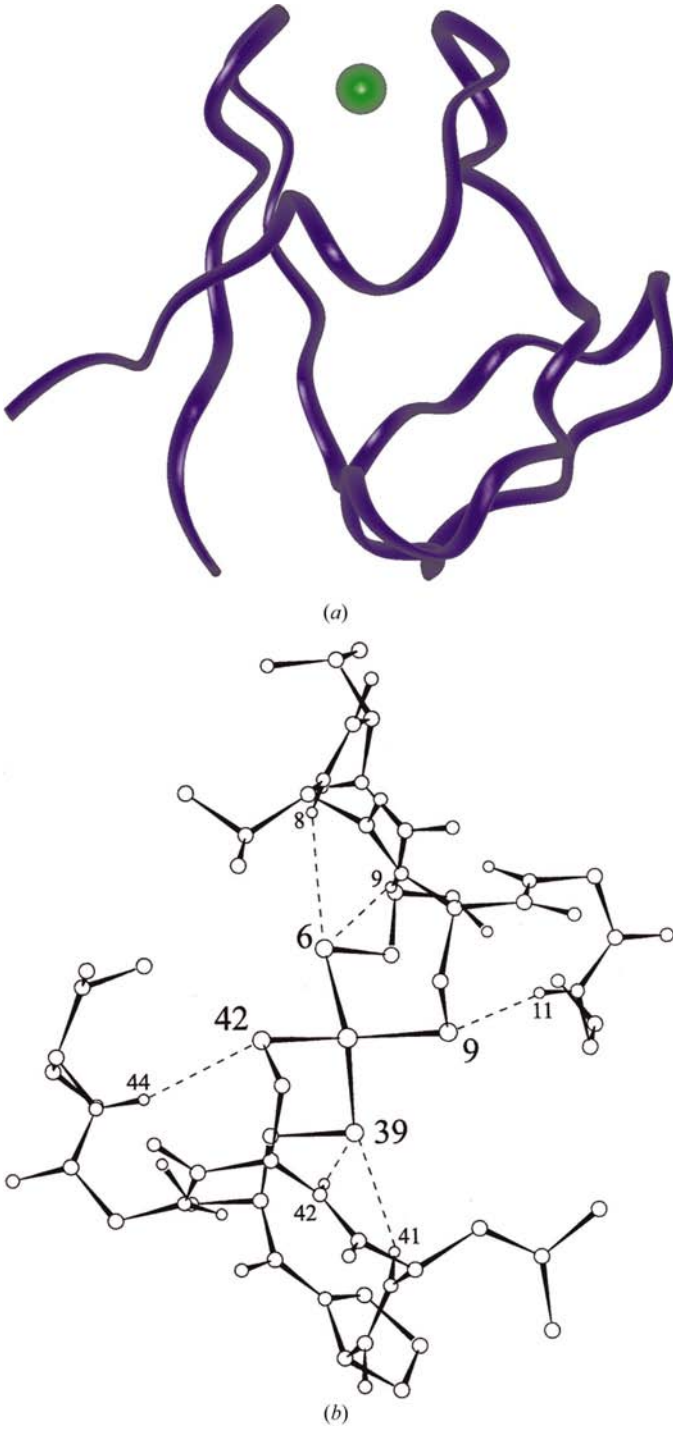

Figure 1
Structure of the rubredoxin from *C. pasteurianum*. (*a*) Overall structure (based on PDB code 1iro). The protein backbone is represented as a blue ribbon and the Fe atom as a green sphere. (*b*) NH···S interactions (dashed lines) around the $Fe(S\text{-}Cys)_4$ centre in Rd*Cp* (generated from the coordinates of PDB code 5rxn). A pseudo-twofold axis is perpendicular to the page, passing through the Fe atom (centre). Numbered amino acids correspond to the following: Cys6, Val8, Cys9, Tyr11, Cys39, Ile41, Cys42 and Val44.

(iii) The so-called 'Rd-knuckle' fold has been recognized as a common structural motif for zinc-finger proteins (Krishna *et al.*, 2003; Wang *et al.*, 2003), for which the crystal structure of Zn-substituted Rd*Cp* has been employed as a high-resolution model (PDB code 1irn; 1.2 Å; Dauter *et al.*, 1996). In this context, the propensity of Rd*Cp* to bind zinc has been examined. Rubredoxin expresses as a mixture of Fe and Zn centres in *Escherichia coli* (Eidsness *et al.*, 1992; Mathieu *et al.*, 1992) and this aspect has been studied directly using electrospray ionization–Fourier transform ion cyclotron resonance (ESI–FTICR) mass spectrometry (Taylor *et al.*, 2001). This work indicated that FeRd and ZnRd are produced simultaneously during overexpression, but at different rates. ZnRd concentrations continued to increase after the cessation of FeRd production owing to the consumption of available iron. The mechanisms for selective iron incorporation into Rd in its native organisms remain unknown.

The ability of Rd to bind transition metals other than iron and the effects on its properties and structure have been explored (May & Kuo, 1978; Moura *et al.*, 1991; George *et al.*, 1996). Of particular note was the work of Archer *et al.* (1995, 1999) on the structures of metal-substituted forms of the rubredoxin-like protein desulforedoxin from *D. gigas*. Structures featuring the pairs of congeners (Ga^{III}, In^{III}) and (Cd^{II}, Hg^{II}) were reported to 1.9, 1.8, 2.0 and 2.5 Å resolution, respectively. The results showed that overall the secondary and tertiary structures of the protein were maintained regardless of the incorporated metal, but that some differences in metal coordination occurred.

We report here the generation and subsequent determination of the X-ray crystal structures of Cd-, Hg-, Co-, Ni- and Ga-substituted derivatives of Rd*Cp*. The work provides an additional structural resource in understanding the essential chemistry of the Rd active site.

2. Materials and methods

2.1. Protein expression, metal substitution and characterization

The procedures for protein expression and isolation have been described previously and used plasmid pKK223-3/Rd*Cp* in *E. coli* strain JM109 (Ayhan *et al.*, 1996). The pure iron-containing protein preparations were converted to Cd-, Hg-, Co-, Ni- or Ga-substituted forms by denaturation of the protein with acid, followed by refolding in the presence of the new metal. The protein (5 mg, 2 mg ml^{-1}) was precipitated by addition of ∼5–10% trichloroacetic acid (TCA) and 0.15 *M* β-mercaptoethanol. After centrifugation (7600 rev min^{-1}, 3 min), the protein pellet was washed with 5% TCA containing β-mercaptoethanol (0.15 *M*). After twofold dilution with water, the precipitation and dissolution procedure was repeated. The final pH was approximately 8. A twofold molar excess of solutions of the nitrate salts of Cd^{II}, Hg^{II}, Co^{II}, Ni^{II} or Ga^{III} (in water) was added. After incubation on ice

Table 1
Data collection and refinement statistics.

(*a*) Crystallographic data for metal-substituted Rd*Cp* proteins. Values in parentheses are for the highest resolution shell.

	Cd	Hg	Co	Ni	Ga
Colour	Colourless	Colourless	Green	Yellow	Colourless
Unit-cell parameters					
a (Å)	64.52	64.44	64.46	64.33	64.25
c (Å)	32.57	32.59	32.64	32.12	32.85
Resolution (Å)	1.5	1.6	1.7	1.9	1.6
Mosaicity (°)	0.27	0.31	0.41	0.34	0.31
Unique observations	7544	6532	5552	3599	6611
Total observations	29513	16227	16277	8168	17349
Completeness (%)	93.9 (66.4)	98.5 (90.0)	99.7 (99.8)	91.5 (77.3)	99.0 (91.5)
$I/\sigma(I)$	14.5 (1.5)	5.8 (2.4)	11.6 (2.3)	9.7 (2.4)	11.3 (1.6)
Redundancy	3.9 (1.6)	2.1 (1.7)	2.3 (2.2)	1.9 (1.5)	2.2 (1.7)
$R_{\rm merge}$	0.111 (0.120)	0.110 (0.271)	0.064 (0.393)	0.074 (0.379)	0.070 (0.386)

(*b*) Refinement statistics for metal-substituted Rd*Cp* proteins.†

	Cd	Hg	Co	Ni	Ga
Resolution range (Å)	19–1.5	16–1.6	20–1.7	20–2.0‡	19–1.6
No. water molecules	41	52	46	23	36
No. residues with alternative conformations	2	1	2	1	1
No. atoms	468	478	469	452	457
No. reflections	7541	6528	5524	3128	6297
$R_{\rm cryst}$	0.146	0.151	0.145	0.219	0.156
$R_{\rm free}$§	0.146	0.189	0.197	0.242	0.206
R.m.s.d. bond lengths (Å)	0.007	0.008	0.011	0.010	0.010
R.m.s.d. bond angles (°)	1.2	1.3	1.4	1.4	1.6
Mean *B* value (Å^2)	14.6	12.2	20.6	25.5	15.2
B value, metal atom¶ (Å^2)	15.9	18.5	28.5	38.4	16.5
Atomic anisotropy *A*††	0.583	0.372	0.652	0.551	0.583
Ramachandran plot, residues in‡‡					
Most favoured regions (%)	95	95	90	92.5	95
Additional allowed regions (%)	5	5	10	7.5	5
S.u.§§ (Å)	0.04	0.06	0.08	0.12	0.06

† Not all data were used for refinement. No σ cutoff was applied to F_o. ‡ Data used in the refinement were limited to 2.0 Å because of unacceptably high residuals in the highest shell. § 5% of the reflections were reserved for calculation of $R_{\rm free}$. Relative $R_{\rm free}$ values were followed throughout the refinement. Since the $R_{\rm free}$ set typically consisted of 150–350 reflections, its absolute value was used as a guide only. ¶ The application of TLS to the refinement led to relatively lower *B* values for main-chain and side-chain atoms. The higher *B* values for the metal atoms in the CoRd and NiRd structures may reflect less than full occupancy for those metals. †† As calculated by *RASTEP*. *A* is the ratio of the smallest and largest eigenvalues of the atomic displacement matrix. $A = 1.0$ indicates a perfect sphere (Merritt, 1999). ‡‡ Calculated using *PROCHECK* (Laskowski *et al.*, 1993). §§ Estimated s.u. in atomic position, based on maximum likelihood (Murshudov & Dodson, 1997).

Table 2
Molar weights (Da) determined by electrospray ionization mass spectrometry.

	Calculated	Found†
FeRd‡	6100.5	6101 (1)
CdRd‡	6158.7	6159 (1)
HgRd	6246.3	6245 (1)
CoRd	6104.6	6103 (1)
NiRd	6104.4	6104 (1)
GaRd	6115.4	6114 (1)

† Single standard deviations are given in parentheses. ‡ Taken from Ayhan *et al.* (1996).

(1 h), a precipitate was removed by filtration. The solution was diluted fourfold with buffer (50 m*M* Tris–HCl pH 7.8) and applied to a DEAE-52 anion-exchange column (1.5 × 6.0 cm), which had been equilibrated with buffer. The protein was batch-eluted (9–12 ml, ∼0.5 mg ml^{-1}) with a solution of 0.3 *M* NaCl in buffer. The eluted samples were concentrated by centrifugal ultrafiltration. Electrospray ionization mass spectrometry (ESI–MS) was carried out as described previously (Ayhan *et al.*, 1996).

2.2. Crystallization and data collection

All Rd*Cp* derivatives were crystallized by the hanging-drop vapour-diffusion technique. Hanging drops containing protein (4.0 µl, 7–20 mg ml^{-1}) and an equal volume of reservoir solution were suspended above a reservoir (700 µl) containing ammonium sulfate (50–67% saturation at 277 K) and buffer (0.05 *M* sodium acetate pH 4.0–4.6) and were incubated at 277 K. Crystals generally appeared in 2–7 d. In all cases, the crystals were mounted in a glass capillary and data were collected at 293 K on an R-AXIS IIc image-plate detector with Cu $K\alpha$ X-rays from a Rigaku RU-200 rotating-anode generator, focused using mirror optics. The diffraction data were processed and scaled using the programs *DENZO* and *SCALEPACK* (Otwinowski & Minor, 1997). Data-collection statistics are summarized in Table 1(*a*).

2.3. Structure determination and refinement

All forms of Rd*Cp* crystallized in space group *R*3, with similar unit-cell parameters (Table 1*a*). Consequently, the starting model for all five structures was the 1.1 Å Rd*Cp* structure (PDB code 1iro), with the Fe atom and all water molecules omitted. A single cycle of rigid-body refinement was followed by a cycle of positional refinement with *REFMAC*5 (Murshudov *et al.*, 1997). In all five structures, a large positive peak was observed in the difference Fourier electron-density map at the metal-coordination site. The appropriate metal atom was placed on this site and refinement was completed with *REFMAC*5 using TLS (Murshudov *et al.*, 1997). Ordered water molecules were added to all structures automatically using *ARP* and were authenticated manually by inspection of electron-density maps in *O*, with consideration of hydrogen-bonding criteria (Jones *et al.*, 1991). In all cases, the final refinement cycle included anisotropic displacement parameter refinement of the metal atom (Murshudov *et al.*, 1999). Structures were validated using *PROCHECK* (Laskowski *et al.*, 1993). Estimated standard uncertainties (s.u.) in atomic positions, based on maximum likelihood, were calculated in *REFMAC*5 (Table

Table 3
Comparisons of the structures of metal-substituted rubredoxins.

	FeRd†	ZnRd†	CdRd	HgRd	CoRd	NiRd	GaRd
R.m.s.d. 53 C^{α} atoms (Å)		0.12	0.13	0.13	0.15	0.16	0.13
Bond distances (Å) (differences from FeRd indicated in parentheses)							
6 S^{γ}—*M*	2.287	2.365 (+0.078)	2.52 (+0.23)	2.66 (+0.37)	2.33 (+0.04)	2.25 (−0.04)	2.32 (+0.03)
9 S^{γ}—*M*	2.249	2.331 (+0.082)	2.50 (+0.25)	2.40 (+0.15)	2.26 (+0.01)	2.38 (+0.13)	2.29 (−0.04)
39 S^{γ}—*M*	2.283	2.368 (+0.085)	2.55 (+0.27)	2.57 (+0.29)	2.32 (+0.04)	2.48 (+0.20)	2.31 (−0.03)
42 S^{γ}—*M*	2.230	2.313 (+0.084)	2.46 (+0.23)	2.34 (+0.11)	2.24 (+0.01)	2.13 (−0.10)	2.25 (+0.02)
Mean s.u.‡	0.003†	0.004†	0.05	0.08	0.11	0.18	0.08
Bond angles (°) (differences from FeRd indicated in parentheses)							
6 S^{γ}—*M*—9 S^{γ}	113.4	113.0 (−0.4)	110.9 (−2.5)	108.1 (−5.3)	113.3 (−0.1)	121.4 (+8.0)	113.7 (+0.3)
6 S^{γ}—*M*—39 S^{γ}	110.1	111.9 (+1.8)	113.4 (+3.3)	107.8 (−2.3)	110.6 (+0.5)	116.0 (+5.9)	109.8 (−0.3)
6 S^{γ}—*M*—42 S^{γ}	104.3	104.5 (+0.2)	105.8 (+1.5)	107.5 (+3.2)	104.9 (+0.6)	105.1 (+0.8)	103.5 (−0.8)
9 S^{γ}—*M*—39 S^{γ}	104.6	104.1 (−0.5)	105.0 (+0.4)	107.1 (+2.5)	104.6 (0.0)	101.8 (−2.8)	103.3 (−1.3)
9 S^{γ}—*M*—42 S^{γ}	112.7	111.8 (−0.9)	110.0 (−2.7)	112.4 (−0.3)	108.8 (−3.9)	104.1 (−8.6)	112.3 (−0.4)
39 S^{γ}—*M*—42 S^{γ}	111.9	111.7 (−0.2)	110.9 (−1.0)	113.8 (+1.9)	114.8 (+2.9)	107.1 (−4.8)	114.5 (+2.6)
Mean s.u.‡	0.1†	0.1†	1.9	2.8	4.3	7.0	4.6
Hydrogen-bonding distances (Å) (differences from FeRd indicated in parentheses)							
6 $S^{\gamma}\cdots$N8	3.677	3.571 (−0.106)	3.52 (−0.16)	3.57 (−0.11)	3.63 (−0.05)	3.63 (−0.05)	3.66 (−0.02)
6 $S^{\gamma}\cdots$N9	3.646	3.501 (−0.145)	3.52 (−0.13)	3.61 (−0.04)	3.62 (−0.03)	3.67 (+0.02)	3.65 (0.00)
9 $S^{\gamma}\cdots$N11	3.488	3.454 (−0.034)	3.43 (−0.06)	3.49 (0.00)	3.54 (+0.05)	3.54 (+0.05)	3.50 (+0.12)
39 $S^{\gamma}\cdots$N41	3.541	3.432 (−0.109)	3.44 (−0.10)	3.45 (−0.09)	3.45 (−0.09)	3.51 (−0.03)	3.53 (−0.01)
39 $S^{\gamma}\cdots$N42	3.578	3.553 (−0.025)	3.62 (+0.04)	3.65 (+0.07)	3.59 (+0.01)	3.58 (0.00)	3.61 (+0.03)
42 $S^{\gamma}\cdots$N44	3.844	3.764 (−0.080)	3.80 (−0.04)	3.92 (+0.08)	3.88 (+0.04)	4.08 (+0.24)	3.89 (+0.05)

† Taken from Dauter *et al.* (1996). ‡ Calculated using the s.u. in atomic position, based on maximum likelihood (Table 1*b*; Murshudov & Dodson, 1997).

1*b*; Murshudov & Dodson, 1997; Murshudov *et al.*, 1997). This method uses an extension of the fundamentals of the dispersion precision indicator (DPI; Cruickshank, 1999). These uncertainties were used to estimate conservatively the errors in bond lengths and angles. Refinement statistics are detailed in Table 1(*b*).

3. Results and discussion

By denaturation of the protein in the presence of acid, followed by refolding, the active-site Fe atom of Rd*Cp* was successfully replaced in turn with Co^{II}, Ni^{II}, Ga^{III}, Cd^{II} and Hg^{II} (Moura *et al.*, 1991; Xiao *et al.*, 1998). All five derivatives of the protein were stable under aqueous conditions at ambient temperature. ESI–MS analysis of the metal-substituted Rd*Cp* solutions confirmed the incorporation of the new metal and the absence of iron-containing or metal-free forms (Table 2). Each protein crystallized under conditions modified from that for native Rd*Cp*, in space group *R*3, and all were isomorphous with the native Rd*Cp* structure (PDB code 1iro; Dauter *et al.*, 1996). The resolution limits of the refined structures range from 1.5 to 2.0 Å (Table 1*b*). An initial round of positional refinement of the metal- and water-free Rd*Cp* coordinates against the data of the respective metal-substituted proteins led to a significant positive difference Fourier electron-density peak in each metal site. The intensities of these peaks were approximately 19, 12, 31, 44 and 38σ for the Co-, Ni- Ga-, Cd- and Hg-substituted proteins, respectively, which correlate reasonably with the atomic number of each metal (Co 27, Ni 28, Ga 31, Cd 48 and Hg 80). All structures refined to acceptable residuals, with little geometric distortion (Table 1*b*). Refinement of the individual anisotropic displacement parameters of the active-site metals assisted in eliminating residual difference Fourier electron density from each metal site. This refinement technique revealed some anisotropy associated with the metal atoms in all structures (Table 1*b*), with the Hg^{II} atom in the HgRd structure being the least isotropic.

A comparison of the structures of the Co^{II}-, Ni^{II}-, Ga^{III}-, Cd^{II}- and Hg^{II}-substituted Rd proteins against the previously reported structures of the native Fe^{III}- and the Zn^{II}-substituted proteins is detailed in Table 3. Least-squares superposition of each structure with that of Fe^{III}Rd resulted in r.m.s. deviations in 53 C^{α} positions between pairs of structures of 0.12–0.16 Å. These distortions are clearly small and indicate that the overall structure of Rd*Cp* is unaffected by the identity of the incorporated metal. Any structural distortions are confined to the metal-coordination sites, specifically the metak–sulfur bond lengths and associated angles.

The Fe^{III}-coordination site in native Rd*Cp* shows approximate D_{2d} symmetry, distorted from tetrahedral geometry by compression along the S_4 axis. The Fe—S bond lengths are divided into two longer (Cys6 S^{γ}—Fe and Cys39 S^{γ}—Fe) and two shorter (Cys9 S^{γ}—Fe and Cys42 S^{γ}—Fe) distances. Correspondingly, two S—Fe—S angles (6 S^{γ}—*M*—42 S^{γ} and 6 S^{γ}—*M*—42 S^{γ}) are more acute than the other four (Table 3). For the Co^{II}- and Ga^{III}-substituted proteins, the metal sites were indistinguishable from the Fe^{III} case. The resolution of 2.0 Å for the Ni-substituted Rd*Cp* structure is lower than those of the other structures. Consequently, the estimated s.u. associated with the atomic positions is significantly higher (0.12 Å). Two *M*—S bond lengths may differ significantly from the Fe^{III} case, but further discussion must await a structure of higher precision.

For Cd^{II}Rd, the *M*—S bond lengths are on average 0.25 (5) Å longer than those in the Fe^{III}Rd protein, consistent

with the different four-coordinate ionic radii of the two metals (0.92 and 0.63 Å for Cd^{II} and Fe^{III}, respectively; Huheey *et al.*, 1993). As the observed changes in S—*M*—S angles are close to the limits of precision, substitution of Cd^{II} for Fe^{III} has led to an isotropic expansion of the metal-coordination sphere with overall conservation of geometry. The NH···S hydrogen-bond lengths responded by decreasing by an average of 0.08 (5) Å, with the largest changes observed for the 6 S^{γ}···N8 and 6 S^{γ}···N9 interactions.[1] A similar expansion of the metal coordination site was observed for the Hg^{II}-substituted protein. The average increase in *M*—S bond length from that observed for FeRd is 0.23 (8) Å. As for the Fe protein, the Cys6 S^{γ}—Hg and Cys39 S^{γ}—Hg bonds are longer than the Cys9 S^{γ}—Hg and Cys42 S^{γ}—Hg bonds. The differences between these pairs of distances is pronounced, however, at ∼0.25 Å. Most changes in the S—Hg—S bond angles are close to experimental error. This disparity between the Cys6/39 S^{γ}—Hg and Cys9/42 S^{γ}—Hg bond lengths has not been observed previously. George *et al.* (1996) used X-ray absorption spectroscopy to examine the metal-site structures of Fe^{II}-, Fe^{III}-, Zn^{II}- and Hg^{II}-rubredoxins from *P. furiosus*. The average Hg—S bond length for the Hg-substituted protein was 2.534 (2) Å, which agrees well with the average bond length for HgRd reported here [2.49 (8) Å]. These authors did not, however, observe any evidence for two different pairs of Hg—S distances. In terms of average Hg—S distances, our results also agree with those of Archer *et al.* (1999) for the Hg-substituted desulforedoxin. This structure showed all four Hg—S bond lengths to be approximately equal.

4. Conclusions

The Rd scaffold designates a metal site with essentially tetrahedral geometry and its ability to accommodate a metal with different geometrical preferences is limited. Metals that have a preference for tetrahedral coordination, such as Fe, Co, Zn, Ga and Cd (Holm *et al.*, 1996), bind to the metal coordination site of Rd*Cp* with similar geometries. An increase in the *M*—S bond lengths is observed in the case of Cd substitution because of the larger ionic radius of Cd. Both Ni^{II} and Hg^{II} appear to occupy distorted sites and repeated attempts to incorporate Cu^{II} (with a preference for square-planar coordination) into Rd*Cp* failed (data not shown). The mechanisms by which selective incorporation of Fe (over Zn in particular) into Rd*Cp* is achieved when it is expressed in its native organism remain unknown, particularly when there is no clear geometric distinction between the two metals and Zn is found in greater cellular abundance than Fe (*e.g.* in *E. coli*; D'Souza & Holz, 1999).

In addition, the present work shows Ga to be a better mimic of Fe than Cd in terms of conservation of structure. The presence of paramagnetic Fe^{III} in the metal site of proteins such as Rd leads to difficulties in the application of structural techniques such as NMR. Consequently, diamagnetic metals such as Cd are often substituted for Fe. The ^{113}Cd isotope has a nuclear spin of 1/2 and can be used to measure structural information about the metal site. The present work shows that the incorporation of Cd leads to significant expansion of the metal-binding site of Rd*Cp*. Since Ga is also diamagnetic and its substitution for Fe leads to conservation of metal-site structure, it may be a better choice.

Dr Zhiguang Xiao is thanked for his guidance in the preparation of the metal-substituted Rd*Cp* proteins. This work was supported by Australian Research Council grants A10020211 to AGW and DP0209273 to JMG, and an Australian postdoctoral fellowship (F10009015) to MJM.

References

Archer, M., Carvalho, A. L., Teixeira, S., Moura, I., Moura, J. J., Rusnak, F. & Romao, M. J. (1999). *Protein Sci.* **8**, 1536–1545.
Archer, M., Huber, R., Tavares, P., Moura, I., Moura, J. J., Carrondo, M. A., Sieker, L. C., LeGall, J. & Romao, M. J. (1995). *J. Mol. Biol.* **251**, 690–702.
Ayhan, M., Xiao, Z., Lavery, M. J., Hamer, A. M., Nugent, K. W., Scrofani, S. D. B., Guss, J. M. & Wedd, A. G. (1996). *Inorg. Chem.* **35**, 5902–5911.
Chen, J. C. & Mortenson, L. E. (1992). *Biochim. Biophys. Acta*, **1131**, 122–124.
Cross, M., Xiao, Z., Maes, E. M., Czernuszewicz, R. S., Drew, S. C., Pilbrow, J. R., George, G. N. & Wedd, A. G. (2002). *J. Biol. Inorg. Chem.* **7**, 781–790.
Cruickshank, D. W. J. (1999). *Acta Cryst.* D**55**, 583–601.
Dauter, Z., Wilson, K. S., Sieker, L. C., Moulis, J. M. & Meyer, J. (1996). *Proc. Natl Acad. Sci. USA*, **93**, 8836–8840.
D'Souza, V. M. & Holz, R. C. (1999). *Biochemistry*, **38**, 11079–11085.
Eidsness, M. K., Burden, A. E., Richie, K. A., Kurtz, D. M. Jr, Scott, R. A., Smith, E. T., Ichiye, T., Beard, B., Min, T. & Kang, C. (1999). *Biochemistry*, **38**, 14803–14809.
Eidsness, M. K., O'Dell, S. E., Kurtz, D. M. Jr, Robson, R. L. & Scott, R. A. (1992). *Protein Eng.* **5**, 367–371.
Geissdorfer, W., Frosch, S. C., Haspel, G., Ehrt, S. & Hillen, W. (1995). *Microbiology*, **141**, 1425–1432.
George, G. N., Pickering, I. J., Prince, R. C., Zhou, Z. H. & Adams, M. W. W. (1996). *J. Bioinorg. Chem.* **1**, 226–230.
Gomes, C. M., Silva, G., Oliveira, S., LeGall, J., Liu, M. Y., Xavier, A. V., Rodrigues-Pousada, C. & Teixeira, M. (1997). *J. Biol. Chem.* **272**, 22502–22508.
Herriott, J. R., Sieker, L. C., Jensen, L. H. & Lovenberg, W. (1970). *J. Mol. Biol.* **50**, 391–406.
Holm, R. H., Kennepohl, P. & Solomon, E. I. (1996). *Chem. Rev.* **96**, 2239–2314.
Huheey, J. E., Keiter, E. A. & Keiter, R. L. (1993). *Inorganic Chemistry*, 4th ed., pp. 114–117. New York: Harper Collins.
Jenney, F. E. Jr, Verhagen, M. F., Cui, X. & Adams, M. W. (1999). *Science*, **286**, 306–309.
Jones, T. A., Zou, J.-Y., Cowan, S. W. & Kjeldgaard, M. (1991). *Acta Cryst.* A**47**, 110–119.
Krishna, S. S., Majumdar, I. & Grishin, N. V. (2003). *Nucleic Acids Res.* **31**, 532–550.
Laskowski, R. A., MacArthur, M. W., Moss, D. S. & Thornton, J. M. (1993). *J. Appl. Cryst.* **26**, 283–291.
Lin, I. J., Gebel, E. B., Machonkin, T. E., Westler, W. M. & Markley, J. L. (2003). *J. Am. Chem. Soc.* **125**, 1464–1465.
Lovenberg, W. & Sobel, B. E. (1965). *Proc. Natl Acad. Sci. USA*, **54**, 193–199.

[1] We have reported preliminary details of the CdRd structure previously, citing the average contraction in NH···S bond distances as 0.17 (6) Å (Ayhan *et al.*, 1996). Subsequent refinement has confirmed that the NH···S distances decrease on average, but by a smaller value.

Maher, M. J., Xiao, Z., Wilce, M. C., Guss, J. M. & Wedd, A. G. (1999). *Acta Cryst.* D**55**, 962–968.
Mathieu, I., Meyer, J. & Moulis, J. M. (1992). *Biochem. J.* **285**, 255–262.
May, S. W. & Kuo, J. Y. (1978). *Biochemistry*, **17**, 3333–3338.
Merritt, E. A. (1999). *Acta Cryst.* D**55**, 1109–1117.
Meyer, J., Gaillard, J. & Lutz, M. (1995). *Biochem. Biophys. Res. Commun.* **212**, 827–833.
Moura, I., Teixeira, M., LeGall, J. & Moura, J. J. (1991). *J. Inorg. Biochem.* **44**, 127–139.
Murshudov, G. N. & Dodson, E. J. (1997). *CCP4 Newsl. Protein Crystallogr.* **33**, 31–39.
Murshudov, G. N., Vagin, A. A. & Dodson, E. J. (1997). *Acta Cryst.* D**53**, 240–255.
Murshudov, G. N., Vagin, A. A., Lebedev, A., Wilson, K. S. & Dodson, E. J. (1999). *Acta Cryst.* D**55**, 247–255.
Otwinowski, Z. & Minor, W. (1997). *Methods Enzymol.* **276**, 307–326.
Taylor, P. K., Parks, B. A., Kurtz, D. M. Jr & Amster, I. J. (2001). *J. Biol. Inorg. Chem.* **6**, 201–206.
Wang, B., Alam, S. L., Meyer, H. H., Payne, M., Stemmler, T. L., Davis, D. R. & Sundquist, W. I. (2003). *J. Biol. Chem.* **278**, 20225–20234.
Watenpaugh, K. D., Sieker, L. C., Herriott, J. R. & Jensen, L. H. (1972). *Cold Spring Harb. Symp. Quant. Biol.* **36**, 359–367.
Watenpaugh, K. D., Sieker, L. C. & Jensen, L. H. (1979). *J. Mol. Biol.* **131**, 509–522.
Xiao, Z., Lavery, M. J., Ayhan, M., Scrofani, S. D. B., Wilce, M. C. J., Guss, J. M., Tregloan, P. A., George, G. N. & Wedd, A. G. (1998). *J. Am. Chem. Soc.* **120**, 4135–4150.
Xiao, Z., Maher, M. J., Cross, M., Bond, C. S., Guss, J. M. & Wedd, A. G. (2000). *J. Biol. Inorg. Chem.* **5**, 75–84.
Xiao, Z. & Wedd, A. G. (2001). *Modern Coordination Chemistry – The Legacy of Joseph Chatt*, edited by G. J. Leigh & N. Winterton, pp. 288–302. Cambridge: Royal Society of Chemistry.

Acta Crystallographica Section D
Biological Crystallography
ISSN 0907-4449

addenda and errata

Metal-substituted derivatives of the rubredoxin from *Clostridium pasteurianum*. Addendum

Megan Maher,[a]* Maddalena Cross,[b] Matthew C. J. Wilce,[a] J. Mitchell Guss[a] and Anthony G. Wedd[b]

[a]School of Molecular and Microbial Biosciences, University of Sydney, New South Wales 2006, Australia, and [b]School of Chemistry, University of Melbourne, Parkville, Victoria 3010, Australia. Correspondence e-mail: m.maher@mmb.usyd.edu.au

In our recent article Maher *et al.* (2004) we omitted to cite the work of Meyer *et al.* (1997) who were the first to construct an Fe_2S_2 centre in rubredoxin. This work was later extended in Cross *et al.* (2002), with the construction of other altered metal sites.

References

Cross, M., Xiao, Z., Maes, E. M., Czernuszewicz, R. S., Drew, S. C., Pilbrow, J. R., George, G. N. & Wedd, A. G. (2002). *J. Biol. Inorg. Chem.* **7**, 781–790.
Maher, M., Cross, M., Wilce, M. C. J., Guss, J. M. & Wedd, A. G. (2004). *Acta Cryst.* D**60**, 298–303.
Meyer, J., Gagnon, J., Gaillard, J., Lutz, M., Achim, C., Munck, E., Petillot, Y., Colangelo, C. M. & Scott, R. A. (1997). *Biochemistry*, **36**, 13374–13380.

  DOI: 10.1107/S0907444904004998